

Generation of picoseconds stimulated Raman scattering in a BaWO₄ crystal and frequency up-conversion by difference-frequency generation in BBO

Q.L. Zhang · J. Zhang · S.F. Du · D.X. Zhang ·
B.H. Feng · J.Y. Zhang · J.C. Zang

Received: 11 February 2010 / Revised version: 11 May 2010 / Published online: 30 June 2010
© Springer-Verlag 2010

Abstract The characters of stimulated Raman scattering of BaWO₄ crystal excited by a picoseconds laser at 1064 nm are studied based on optical parametric amplification (OPA). Up to six-order Stokes components and five-order anti-Stokes components are observed. The SRS components are amplified by an OPA and the wavelength tunable range from 411 to 2594 nm is achieved with a maximum conversion efficiency of 38% using the OPA stage.

1 Introduction

Stimulated Raman scattering (SRS) is an inelastic scattering process, where the wavelength the pumped light is converted to another wavelength, accompanied by the excitation of an internal mode of the Raman medium. Therefore, SRS can be used to extend the spectral region of solid-state laser sources and has become a significant nonlinear frequency conversion technique. In the past several years, many Raman crystals have been developed and studied including nitrates [Ba(NO₃)₂], alcites [CaCO₃], iodates [LiIO₃], tungstates [KGd(WO₄)₂, BaWO₄, PbWO₄], and vanadates

[YVO₄ and GdVO₄] [1–3]. Among these Raman crystals, BaWO₄ is considered to be one of the most promising materials for its high gain coefficient in both the steady [4] and the transient states [5]. Li Fan et al. have reported a high-efficiency cw Raman conversion with a BaWO₄ Raman crystal in a diode-end-pumped Nd:YVO₄ laser [6]. P. Černý et al. demonstrated highly efficient SRS in the near-infrared, visible, and UV picoseconds-laser pulses in BaWO₄ crystal [7]. However, a rather limited number of Stokes and anti-Stokes components are generated when it is pumped at 1064 nm. P. Černý et al. reported the observation of the first-, second-, third-order Stokes components and the first-anti-Stokes frequency components [8]. In this paper, very rich SRS spectra pumped by a ps laser at 1064 nm are observed and the spectra include as many as six-order Stokes components and the five-order anti-Stokes frequency components.

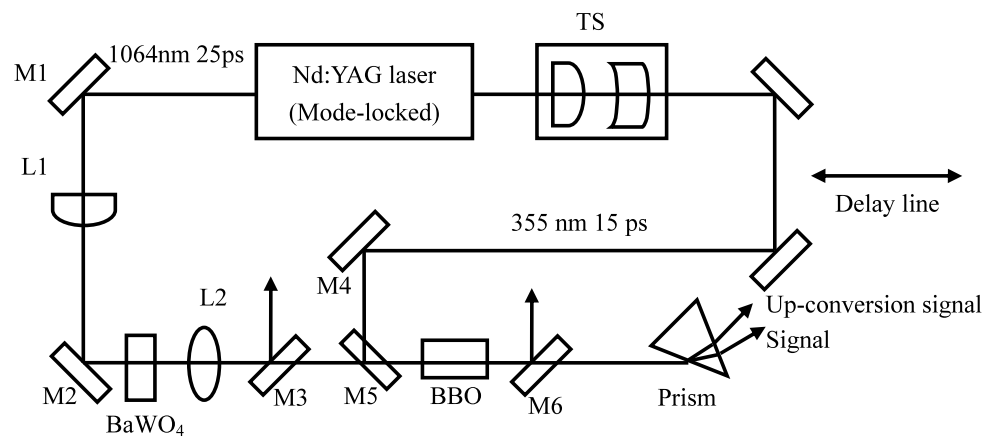
Unfortunately, the intensities of the spectral components obtained in our experiment in the near-infrared are rather weak and most of the optical detectors are unavailable for weak signal in the near-infrared. In recent years, the OPA technique with a high optical gain has been adopted to amplify weak incoherent and coherent light pulses [9–17]. Furthermore, the advantage of the OPA is that it not only directly amplifies the weak light pulses but also converts the optical pulses in the near-infrared or mid-infrared into the visible range through the idler-to-signal up-conversion [16]. Hence OPA is a powerful tool in detecting weak optical signals. In this paper, we demonstrate sensitive detection of the SRS in a BaWO₄ crystal pumped with a laser at 1064 nm. Multi-frequency SRS pulses are generated in the BaWO₄, whose wavelength region is ranging from 713 to 2594 nm. Moreover, the wavelength region is further extended to the region of 411–2594 nm by means of parametric up-conversion of an OPA. The OPA is a nonlinear op-

Q.L. Zhang · J. Zhang · S.F. Du · D.X. Zhang · B.H. Feng (✉)
Laboratory of Optical Physics, Institute of Physics, Chinese
Academy of Sciences, Beijing 100190, China
e-mail: bhfeng@aphy.iphy.ac.cn
Fax: +86-10-82649009

J.Y. Zhang
Department of Physics, Georgia Southern University, Statesboro,
GA 30460, USA

J.C. Zang
College of Materials Science and Engineering, Beijing University
of Technology, Beijing 100022, China

Fig. 1 Schematic diagram of the experimental arrangement: TS1-2, telescope; M1-3, mirrors (highly reflective at 1064 nm); BC, BaWO₄ crystal; L1, lens; M4-6, mirrors (highly reflective at 355 nm)



tical process, in which the strong pumping beam at higher frequency interacts with an optical signal beam at lower frequency and generates a third beam through difference-frequency generation (DFG). If the frequency of the signal beam is lower than the degenerate point or half of the frequency of the pump, the frequency of the generated third beam would be higher than that of the signal and the process is called parametric up-conversion. For our 355-nm-pumped OPA the degenerate point is at 710 nm, therefore, the SRS lines generated by the pump beam at 1064 nm can be mixed with the pump beam at 355 nm, they can be amplified and generate new frequency components through DFG. If the SRS component is on the red side of 710 nm, it acts as the idler beam in the OPA and the generated DFG component is frequency up-converted to the visible as the signal beam. On the other hand, if the anti-Stokes component is in the visible, it acts as the signal beam in the OPA and the DFG generated beam is frequency down-converted to the IR.

2 Experimental arrangements

The schematic diagram of the experimental arrangement is shown in Fig. 1. A repetition rate of 10 Hz passive-active mode-locked Nd:YAG laser (EKSPLA:PL2143B) delivering pulses at 1064 nm (s-polarized, 25 ps) is used as the excitation source of SRS. To increase the pump intensity, the beam's diameter is reduced to approximately 2 mm by a lens at the input face of BaWO₄ crystal. The BaWO₄ crystal is 5 mm in length. The separation of the SRS components from the excitation beam is achieved through a dichroic mirror M3, which is highly reflective at 1064 nm and transparent for the SRS components. The SRS pulses are then seeded into a 355-nm pumped type-I phase-matched BBO crystal after having been collected and collimated by lens L2 ($\Phi = 25.4$ mm, $f = 50$ mm). The BBO crystal is cut at $\theta_c = 28.5^\circ$, $\phi_c = 0^\circ$ with dimensions of 5 mm \times 8 mm \times 11 mm, which is used as the energy amplifier for the SRS pulses. The

third harmonics of the picoseconds Nd:YAG laser (355 nm, p-polarized, 15 ps) is used as the pump source for the BBO-OPA. The diameter of the pump beam at 355 nm is reduced to 3-mm by a telescope. The pump and seed beams are combined collinearly by a dichroic mirror M5, which is highly reflective at 355 nm. The temporal overlap between the seed and the pump pulses is satisfied by precise adjustment of an optical delay line. Behind the BBO crystal, the residual pump pulse at 355 nm is removed by another dichroic mirror M6, which is same as M5. The SRS seed pulses are selectively amplified by rotating the BBO crystal in the perpendicular plane to achieve phase matching. The output of the amplified signal and the parametric up-converted optical pulses are separated by a prism and detected with an energy meter.

3 Results and discussion

3.1 SRS generation

By using the experimental setup, the SRS is generated by firing the fundamental laser beam at 1064 nm onto the BaWO₄ crystal. When the intensity of the excitation beam reaches the SRS threshold, the first-stokes radiation wavelength is measured to be 1180 nm. Increasing the pump intensity, the higher-order Stokes and anti-Stokes lines can be obtained. Figure 2 illustrates the spectra profile of SRS measured by a spectrometer (SpectraPro-500i) and a fiber spectrometer (Ocean Optics, HR2000). In Fig. 2, the highest order anti-Stokes and Stokes lines are the fifth (713 nm) and the second (1324 nm), respectively. The third- (1509 nm), the fourth- (1753 nm), the fifth- (2092 nm) and the sixth-Stokes (2594 nm) are beyond the spectral range of the spectrometers and therefore they are not displayed in Fig. 2. However, the higher-order Stokes lines can be detected by the parametric frequency up-conversion using an OPA stage, which will be described in the following section.

Table 1 Thresholds for the Stokes and anti-Stokes lines in different axes (The fifth, fourth, third, second, first anti-Stokes, first, second, fourth, fifth and sixth Stokes are denoted as AS5, AS4, AS3, AS2, AS1, S1, S2, S4, S5, S6)

	Polarized direction	Assignment	Wavelength (nm)	Up-converted wavelength (nm)	Threshold without OPA (GW/cm ²)	Threshold with OPA (GW/cm ²)
c		S6	2594	411	—	7.0
		S5	2092	428	—	5.9
		S4	1753	445	—	5.0
		S2	1324	485	4.3	3.5
		S1	1180	507	3.3	2.0
		AS1	968	560	3.5	3.0
		AS2	889	590	4.7	3.8
		AS3	821	625	5.6	5.0
		AS4	763	663	6.2	5.6
		AS5	713	707	6.7	—
a		AS1	968	560	6.0	—
		AS2	889	590	6.6	—
		AS3	821	625	7.1	—
		AS4	763	663	7.9	—

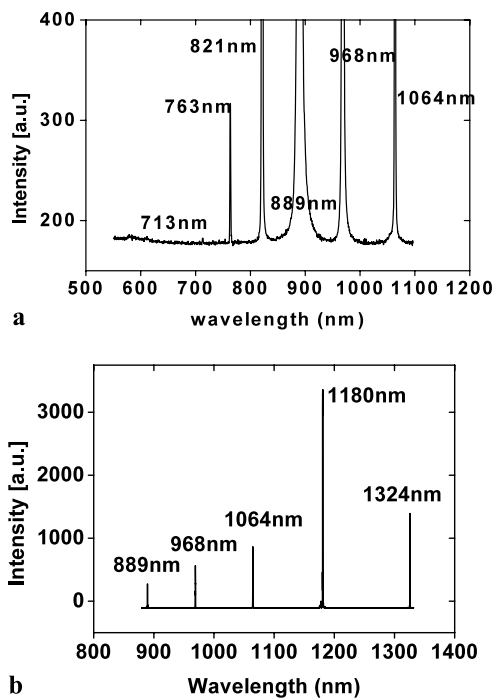


Fig. 2 (a) Spectral profile of the anti-Stokes measured by a fiber spectrometer (Ocean Optics, HR2000); (b) Spectral profile of the Stokes measured by a spectrometer (SpectraPro-500i). The excitation beam energy is 7.2 mJ

The thresholds for different Stokes and anti-Stokes lines are measured through observing the spectra of the SRS by using a fiber spectrometer, which are presented in Table 1. As shown in Table 1, the SRS generation thresholds of the a-polarized pump are higher compared with the c-polarized

pump, which is consistent with the earlier experimental result [18].

3.2 Parametric amplification and up-conversion for the SRS pulses

In order to detect the Stokes components, an OPA stage is employed to amplify SRS lines and up-converted SRS lines in the near-infrared range to the visible light. Measurement of the up-converted SRS in the visible light can provide the information on the generation of the higher Stokes lines. Experimentally, each SRS components can be amplified individually by rotating the angle of BBO crystal to achieve phase matching for the specific SRS wavelength. A photograph of the typically amplified first-anti-Stokes line at 968 nm is shown in Fig. 3. As can be seen from the figure, the amplified SRS laser has a good beam quality.

Figure 4 displays the spectrum of parametrically up-converted signal at 411 nm corresponding to the SRS wavelength at 2594 nm. The spectral profile of the amplified signal is recorded by a spectrometer (Ocean Optics, HR2000). First, the parametric fluorescence generated by the pump at 355-nm is recorded as a background by a spectrometer with the excitation source of 1064 nm is blocked. Then the spectral profile of the amplified signal is recorded with the excitation source of 1064 nm is unblocked so that the OPA is seeded with SRS component. A strong beam at 411 nm can be measured. It is attributed to DFG between the pump at 355 nm and the SRS component at 2594 nm and frequency up-conversion. The seeded SRS at 2594 nm cannot be displayed with the CCD spectrometer, whose wavelength range is in the visible and cutoff at >1100 nm. The up-converted line at 411 nm cannot be generated by the DFG between

Table 2 Output energy of the amplified SRS pulses and parametrically up-converted signal (The amplified energy of the other SRS lines is lower than 0.1 mJ)

Assignment	SRS components		Up-converted signal	
	Wavelength (nm)	Energy (mJ)	Wavelength (nm)	Energy (mJ)
AS3	821	0.11	625	0.16
AS2	889	0.15	590	0.21
AS1	968	0.098	560	0.21
S1	1180	0.19	507	0.56
S2	1324	0.1	485	0.21

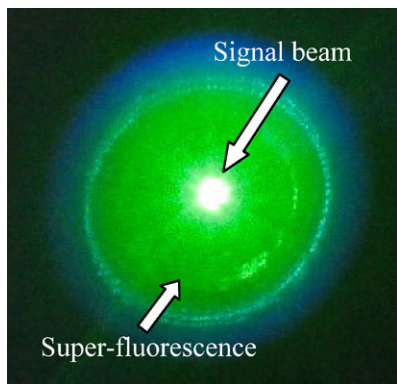


Fig. 3 Photograph of the optical parametric super-fluorescence, the amplified signal spot of the first-anti-Stokes component ($\lambda = 968$ nm) and the up-converted component ($\lambda = 560$ nm) recorded by a common CCD camera

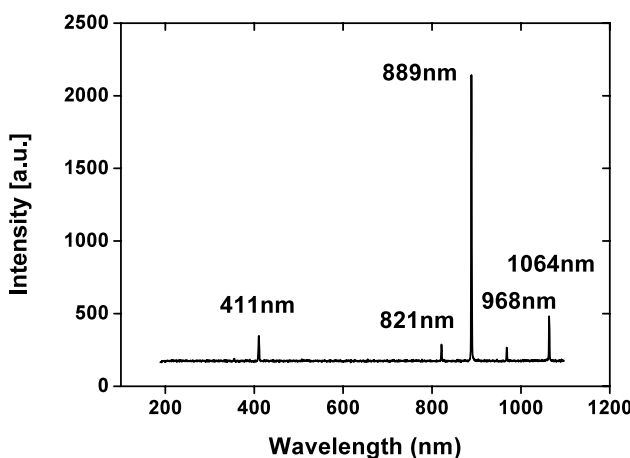


Fig. 4 Parametrically up-converted spectral profile at 411 nm corresponding to the sixth-Stokes wavelength at 2594 nm. The seeded sixth-Stokes line cannot be displayed by the CCD because of the limited spectral range. The pump beam energy of 355 nm is 2 mJ

the pump and the quantum noise, since the generated beam is highly collimated spot, which is very different from the amplified super-fluorescence as can be seen in Fig. 3. The corresponding up-converted lines of the other SRS components are also measured. For the fourth, third, second, first anti-Stokes and first, second, fourth, fifth and sixth Stokes, the corresponding up-converted wavelengths of the 355 nm-

pumped OPA are 663, 625, 590, 560, 507, 484, 445, 428 and 411 nm, respectively. Due to the fifth anti-Stokes (713 nm) is near the degeneracy point of 355 nm pumped OPA, the amplified fifth anti-Stokes is not observed [19]. For the third-Stokes (1509 nm), the incident angle of the laser beam is perpendicular to the input face of the BBO crystal when the phase matching is satisfied. The back reflection of the residual fundamental laser beam from the BBO surface may damage the YAG laser rod. In order to avoid damaging Nd:YAG laser the third-Stokes components is not amplified either.

By using the OPA stage, the thresholds for the generation of SRS components are also measured through observing the spectra of the up-converted signal, which are displayed in Table 1. Compared with the generation thresholds measured by the traditional method without the OPA, the thresholds measured by using the OPA method are much lower as OPA can amplify weak signals.

The energies of the amplified SRS components and the parametrically up-converted signal are measured at the same time and presented in Table 2. The pump energy at 355 nm for OPA is 2 mJ and the excitation energy at 1064 nm for SRS is 7.2 mJ. It can be seen from Table 2 that the maximum output energy is about 0.19 mJ for the amplified first-Stokes line at 1180 nm and 0.56 mJ for the corresponding up-converted signal. This corresponds to a total energy conversion efficiency of 37.5% for the OPA.

In addition, the pulse duration is an important parameter for a short-pulse system. The pulse widths of the seeded AS1 and AS2 are measured by variation of the delay between the pump and seeded pulse. The pulse duration of AS1 and AS2 are about 24 and 23 ps, respectively. It is basically the same as that of the excitation laser pulses.

4 Conclusion

In summary, up to six-order Stokes components and five-order anti-Stokes frequency components of SRS are observed pumped by picoseconds 1064 nm in a BaWO₄ Raman crystal. Very rich SRS spectra prove the BaWO₄ crystal is a promising material as efficient Raman shifter. The SRS lines are amplified and up-converted by an OPA based in a BBO crystal. By using the OPA stage, the thresholds

for the generation of SRS are lower than traditional method. At the same time, 22 spectral lines are obtained by the OPA stage and the maximum wavelength range covers from 411 to 2594 nm, which includes the whole visible and the near/mid-infrared region. With a pump energy of 2 mJ at 355 nm for OPA, the maximum output energies of 0.19 mJ at 1180 nm and of 0.56 mJ for corresponding up-converted signal at 507 nm are achieved. The total conversion efficiency is 38%.

Acknowledgements This work is supported by the National Natural Science Foundation of China under Grant No. 60438020 and the National Basic Research Program of China (2007CB613205).

References

1. H.M. Pask, Prog. Quantum Electron. **27**, 3 (2003)
2. P. Černý, H. Jelímková, P.G. Zverev, T.T. Basiev, Prog. Quantum Electron. **28**, 113 (2004)
3. J.A. Piper, H.M. Pask, IEEE J. Sel. Top. Quantum Electron. **13**, 692 (2007)
4. P.G. Zverev, T.T. Basiev, A.A. Sobol, V.V. Skornyakov, L.I. Ivleva, N.M. Polozkov, V.V. Osiko, Quantum Electron. **30**, 55 (2000)
5. P. Černý, P.G. Zverev, H. Jelímková, T.T. Basiev, Opt. Commun. **177**, 397 (2000)
6. L. Fan, Y. Fan, Y. Li, H. Zhang, Q. Wang, J. Wang, H. Wang, Opt. Lett. **34**, 1687 (2009)
7. P. Černý, H. Jelímková, T.T. Basiev, P.G. Zverev, IEEE J. Quantum Electron. **38**, 1471 (2002)
8. P. Černý, W. Zendzian, J. Jabczynski, H. Jelímkova, J. Sulc, K. Kopczynski, Opt. Commun. **209**, 403 (2002)
9. X. Chen, X. Han, Y. Weng, Appl. Phys. Lett. **89**, 061127 (2006)
10. S. Du, D. Zhang, Y. Shi, Q. Li, B. Feng, J.Y. Zhang, Opt. Commun. **281**, 5014 (2008)
11. J.Y. Zhang, C.K. Lee, J.Y. Huang, C.L. Pan, Opt. Express **12**, 574 (2004)
12. P. Fita, Y. Stepanenko, C. Radzewicz, Appl. Phys. Lett. **86**, 021909 (2005)
13. X.F. Han, X.H. Chen, Y.X. Weng, J.Y. Zhang, J. Opt. Soc. Am. B **24**, 1633 (2007)
14. S. Du, D. Zhang, Y. Shi, Q. Li, B. Feng, X. Han, Y. Weng, Opt. Commun. **282**, 1884 (2009)
15. X.F. Han, Y.X. Weng, R. Wang, X.H. Chen, K.H. Luo, L.A. Wu, J.M. Zhao, Appl. Phys. Lett. **92**, 151109 (2008)
16. S. Du, D. Zhang, Y. Shi, Q. Li, B. Feng, J. Zhang, Opt. Commun. **28**, 2638 (2008)
17. G. Cerullo, S. De Silvestri, Rev. Sci. Instrum. **74**, 1 (2003)
18. H. Yu, D. Hu, H. Zhang, Z. Wang, W. Ge, X. Xu, J. Wang, Z. Shao, M. Jiang, Laser Technol. **39**, 1239 (2007)
19. J.Y. Zhang, Y. Kong, Z. Xu, D. Shen, Appl. Opt. **41**, 475 (2002)